

# A theory for understanding one-photon luminescence from a single plasmonic resonator

Keyu Xia,<sup>1,2,\*</sup> Yingbo He,<sup>2</sup> Hongming Shen,<sup>2</sup> Yuqing Cheng,<sup>2</sup> Qihuang Gong,<sup>2,3</sup> and Guowei Lu<sup>2,†</sup>

<sup>1</sup>ARC Centre for Engineered Quantum Systems, Department of Physics and Astronomy, Macquarie University, NSW 2109, Australia

<sup>2</sup>State Key Laboratory for Mesoscopic Physics, Department of Physics, Peking University, Beijing 100871, China

<sup>3</sup>Collaborative Innovation Center of Quantum Matter, Beijing 100871, China

Photon-luminescence from a noble metal nanoparticle promises important applications in various area and is of interest in the fundamental physics. However, understanding of the one-photon luminescence from metallic nanostructures remains a subject of debate. We model a single gold nanorods as a plasmonic resonator processing the collective free-electron oscillations. Our model is in good agreement with most experimental observations, and provides a consistent explanation for both the anti-Stokes and Stokes photon-luminescence emission. Interestingly, it correctly predicts the shape dependence and the saturation of the photonluminescence. Our experimental observations and our model provide a novel view angle to understand the photonluminescence from metallic nanorods.

PACS numbers: 78.67.Bf, 73.22.Lp, 78.55.-m, 42.50.Pq

## I. INTRODUCTION

Photonluminescence (PL) from plasmonic nanoparticles has received considerable attention as noble metal nanostructures exhibit remarkable optical and physical properties different from those of their bulk counterparts [1–4]. It promises important applications in nanoscale imaging [5–8], sensing [9, 10] and even hybrid quantum systems [11].

Although the one-photon luminescence (one-PL) emission from single noble metal nanorods has been well studied, however its origin remains a subject of debate [2, 3, 12, 13]. Moreover, the main features of the PL, e.g. the enhanced quantum yield (QY), shape dependence and the saturation phenomenon, need proper explanation and require further investigation [14]. In contrast to the Stokes emission in the one-PL, the anti-Stokes emission has a considerably different spectral profile but rarely receives attention. Although it has been observed in the PL of gold nanoparticles a decade ago [15], no explanation has been suggested and little information has been provided for this process. The inertialess frequency up-conversion has been reported by heating the metal into thousands of K with near and far IR lasers [16–18]. The incoherent emission spectrum from this black body radiation has a Planck distribution [16–18] and must be unpolarized. In contrast, the anti-Stokes PL in our experiment is polarized and has a strong dependence on the excitation and detector polarizations [19], which indicates a coherent frequency up-conversion. Very recently, the thermal occupation of electron-hole excitations in Raman scattering has been suggested to understand the anti-Stokes emission [9]. However, the theory is difficult to consistently explain both the anti-Stokes and Stokes components of the PL from the gold nanorods excited by a cw laser (see Fig. 2(A) in [9]). The discrepancy between the prediction of the theory and the experimental measurement can be one order in amplitude for the Stokes emission and even for the anti-Stokes emission in the vicinity of the excitation frequency. Therefore,

to understand the anti-Stokes PL emission requires further investigation.

In this work, we experimentally and theoretically studied the one-photon luminescence from a single gold nanorod excited by a cw laser. We model the PL from the single gold nanorod as the emission from a local surface plasmonic resonance (LSPR) mode. This model provides a self-consistent and unified understanding for both the anti-Stokes and Stokes PL emission. It reveals that the quantum occupation of the free electron state density (FESD) at thermal equilibrium plays a crucial role in the anti-Stokes emission. The FESD distribution in our model is Fermi-Dirac distribution and indicates a fundamental physic mechanism different from the thermal excitation suggested by Huang et al. [9]. Equally important, it provides a good explanation for the main features of previous experimental observations, e.g. the enhanced quantum yield, the saturation and the shape dependence of the one-PL from noble metal nanoparticles.

## II. MODEL

In metallic nanostructures like gold nanorods, the *sp*-band free electrons can interact with photons directly and can be driven by a laser to collectively oscillate. The collective oscillation of free electrons (COoFE) in a metallic nanoparticle has been proved [20, 21]. On the basis of the concept of the COoFE, we present a theoretical model to explain the main features of the PL spectrum from a single gold nanorod under a cw laser excitation. Our model shown by the diagram in Fig. 1 involves four processes: (i) the laser drives the COoFE; (ii) the created COoFE excites the LSPR mode  $\hat{a}_c$  as the input  $\alpha_{in}$ ; (iii) the LSPR mode generates an output  $\alpha_{out}$  of the COoFE surrounding the surface of the nanorod; (iv) the mode-generated COoFE couples to the light and generates the PL. A linear-polarized input laser field  $\vec{E}_{in}e^{-i\omega_{in}t}$  drives the free electrons to collectively oscillate at the frequency  $\omega_{in}$ . The polarization of the COoFE created by the light source is along  $\vec{E}$ . Similar to the nano photonic crystal cavity localizing a quantized electromagnetic field [22], the single metal nanorod supports a local surface plasmonic resonance (LSPR) mode

\* keyu.xia@mq.edu.au

† guowei.lu@pku.edu.cn

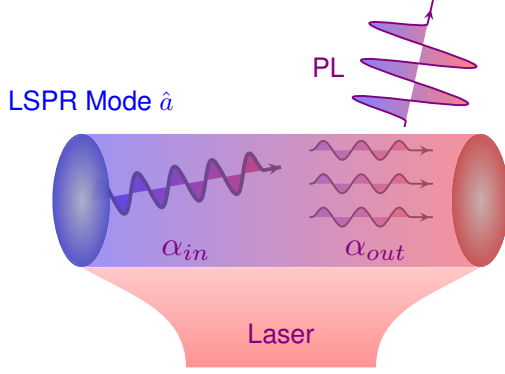


FIG. 1. (Color online) Diagram showing the one-photon luminescence from a single gold nanorod excited by a laser beam. The laser beam drives a collective oscillation of free electrons (COoFE) polarized along the polarization of the light. This electron oscillation as an input  $\alpha_{in}$  subsequently excites the LSPR mode. In return, the LSPR mode generates COoFE as an output  $\alpha_{out}$  and emit the photon-luminescence.

$\hat{a}_c$  polarized along  $\vec{d}$ . The LSPR mode is excited by the collective oscillation of free electrons (COoFE) in the nanorod. Subsequently, the collectively oscillating free-electron gas as an input  $\alpha_{in}$  excites the LSPR mode polarized along  $\vec{d}$ . In return, the LSPR mode generates a COoFE with a polarization of  $\vec{d}$  as an output  $\alpha_{out}$ . As a result, the oscillating free-electron gas emits photon-luminescence (PL). In our model the free electrons gain energy directly from photons but not from the heating effect of the excitation laser [9, 16–18].

The coupling efficiency between the light and the COoFE is proportional with the spatial and temporal overlap of the modes [23, 24]

$$\eta_c(\omega) = \frac{\langle H_{COoFE} | H_{photon} \rangle^2}{|H_{COoFE}|^2 |H_{photon}|^2} \eta_e(\omega),$$

where  $H_{COoFE}$  and  $H_{photon}$  are the profiles of the COoFE and incident light modes. For a given sample,  $H_{COoFE}$  of the SPR mode is fixed. So, the coupling efficiency is determined by the occupation of electrons  $\eta_e(\omega) = |H_{COoFE}|^2$  at the energy  $\hbar\omega$ . The occupation  $\eta_e(\omega)$  is proportional to the total number of electrons,  $N_{FE}$ , attending the collective oscillation and corresponds to the radiation power at the frequency  $\omega$ . Our definition is different from those in [23, 24] because we consider the dependence of  $|H_{COoFE}|^2$  on the energy  $\hbar\omega$  of the sp-band free electrons.

Now we turn to derive the PL spectrum from the Hamiltonian describing the interaction between the light and the plasmon mode  $\hat{a}_c$ . When we apply a cw laser beam to the gold nanorod, the generated sp free-electron gas gaining energy  $\hbar\omega_{in}$  rapidly reaches its thermal equilibrium due to the fast electron-electron and electron-phonon interaction [25, 26]. Therefore, the PL intensity is modulated by the free-electron state density (FESD)  $\eta_e(\omega)$  at the energy  $\hbar\omega$ . In the thermal equilibrium, the FESD follows the Fermi-Dirac statistic dis-

tribution [25, 26]

$$\eta_e(\omega) = N_{FE} / (1 + e^{\hbar(\omega-\mu)/K_B T}), \quad (1)$$

with the so-called chemical potential  $\mu$  [12].  $K_B$  is the Boltzmann constant and  $T$  is the localized temperature. Note that this excitation distribution is essentially different from the thermal occupation suggested by Huang et al. [9]. The motion of the SPR mode can be described using the Hamiltonian

$$H = \omega_c \hat{a}_c^\dagger \hat{a}_c + i \sqrt{2\kappa_{ex1}} (\alpha_{in}^* \hat{a}_c^\dagger - \alpha_{in} \hat{a}_c), \quad (2)$$

where the first term describes the free-energy of the LSPR mode  $\hat{a}_c$  and  $\omega_c$  is the resonance frequency. The COoFE relevant to  $\alpha_{in}$  drives the LSPR mode with a coupling rate  $\kappa_{ex1}$ . Thus, the input  $\alpha_{in}$  is determined by the amplitude of the COoFE and the angle  $\theta$  defined by  $\cos \theta = \vec{E} \cdot \vec{d} / |\vec{E}| |\vec{d}|$  and takes the form

$$\alpha_{in} = \sqrt{\eta_c(\omega_{in})} \cos \theta E_{in} e^{-i\omega_{in} t}. \quad (3)$$

The dynamics of the LSPR mode can be solved by the equation [22, 27, 28]

$$\frac{\partial \hat{a}_c}{\partial t} = -(i\omega_c + \kappa) \hat{a}_c + \sqrt{2\kappa_{ex1}} \sqrt{\eta_c(\omega_{in})} \cos \theta E_{in} e^{-i\omega_{in} t},$$

where  $\kappa$  is the total decay rate of the LSPR mode due to its coupling to the COoFE, the environment and the material absorption. The time-dependent  $\hat{a}_c(t)$  is solved to be

$$\begin{aligned} \hat{a}_c(t) = & \hat{a}_c(0) e^{-(i\omega_c + \kappa)t} - \sqrt{2\kappa_{ex1} \eta_c(\omega_{in})} \cos \theta \frac{E_{in}^* e^{-i\omega_{in} t}}{i\Delta_c + \kappa} \\ & + \sqrt{2\kappa_{ex1} \eta_c(\omega_{in})} \cos \theta \frac{E_{in} e^{-(i\omega_c + \kappa)t}}{i\Delta_c + \kappa}. \end{aligned} \quad (4)$$

The excitation of the LSPR mode includes three contributions. The first term indicates the oscillation due to the initial occupation of the LSPR mode itself. It corresponds to the luminescence spectra excited by a ultrashort laser pulse and has the same spectral profile as the scattering featured by the LSPR mode [3, 29]. It is absent in our case here. The second term origins from the elastic scattering of the input field. We assume that the incident light has a linewidth of  $\gamma_{in}$  spanning a spectrum over  $\delta\lambda_{in}$  that the power spectrum of the input  $\Re \left[ \int_0^\infty \lim_{t \rightarrow \infty} \langle E_{in}^*(t + \tau) E_{in}(t) \rangle e^{-i\omega\tau} d\tau \right] = S_{in}(\omega) \propto I_{in}$ , where  $I_{in} = |E_{in}|^2$  is the intensity of the input laser field.  $\Re[\cdot]$  means the real part of numbers. Because  $\gamma_{in}$  (corresponding to  $\delta\lambda_{in} \sim 0.1$  nm) of the input laser field is much smaller than the decay rate  $\kappa$  of the LSPR modes, this term is very large in the intensity of the PL spectra. But it is usually filtered before entering the detector when measuring the PL emission. On the other hand, this term also responses to the scattering spectra excited by an incoherence white light and has Lorentzian profiles,  $\propto \frac{\kappa^2}{(\omega - \omega_c)^2 + \kappa^2}$ . We are interested in the third term, which corresponds to the PL emission of interest. It includes both the Stokes and anti-Stokes components in the PL spectra.

Using the input-output relation  $\langle \hat{a}_{out} \rangle = \sqrt{2\kappa_{ex2}} \langle \hat{a}_c \rangle$  [30, 31], where  $\langle \hat{Q} \rangle$  estimates the quantum average of operator  $\hat{Q}$

and  $\kappa_{ex2}$  the outgoing coupling, and taking into account the state density of free electrons  $\eta_e(\omega)$ , the optical field emitted by the nanorod takes the form

$$\hat{E}_{out}^\dagger(t) = \sqrt{\eta_c(\omega)} \hat{a}_{out}^\dagger. \quad (5)$$

The light emission from the single gold nanorod can be evaluated by

$$I_{full}(\omega) = \frac{\eta_D(\omega) \cos^2 \beta}{\pi} \Re \left[ \int_0^\infty \lim_{t \rightarrow \infty} \langle E_{out}(\tau + t) E_{out}(t) \rangle e^{-i\omega\tau} d\tau \right]$$

where  $\eta_D(\omega)$  is the quantum efficiency of the detector and  $\beta$  the detection polarization angle between the detector and the polarization of the emitted light. The emission  $I_{full}(\omega)$  includes two contributions: the PL  $I_{PL}(\omega)$  and the scattering  $I_{SC}(\omega)$ .

According to the second term of Eq. 4, the scattering  $I_{SC}$ , which can be obtained experimentally through dark-field white light scattering, reads

$$I_{SC}(\omega) = \frac{4\langle \cos^2 \beta \rangle \langle \cos^2 \theta \rangle \eta_D(\omega) \eta_c(\omega_{in})}{\pi} \eta_c(\omega) \times \frac{\kappa_{ex1} \kappa_{ex2}}{\Delta_c^2 + \kappa^2} \delta(\omega - \omega_{in}) \otimes S_{in}(\omega), \quad (6)$$

where  $\delta(\omega)$  is a delta function of  $\omega$  and  $\otimes$  means the convolution of two functions.  $\langle \cdot \rangle$  evaluates the statistic average value. The power spectrum of the white light is approximately constant. Thus  $I_{SC}(\omega)$  has the Lorentzian profile. Note that  $\eta_c(\omega) \delta(\omega - \omega_{in}) = \eta_c(\omega_{in}) \delta(\omega - \omega_{in})$ .

Different from the scattering, the PL is excited by a narrow band laser pulse. After filtering the input laser field and using the quantum regression theorem [32], we obtain the PL intensity readout by the photon detector as

$$I_{PL}(\omega) = \frac{4 \cos^2 \beta \cos^2 \theta \eta_D(\omega) \eta_c(\omega_{in})}{\pi} \eta_c(\omega) \times \frac{\kappa_{ex1} \kappa_{ex2}}{\Delta_c^2 + \kappa^2} \frac{\kappa}{(\omega - \omega_c)^2 + \kappa^2} \otimes S_{in}(\omega). \quad (7)$$

Because the linewidth  $\gamma_{in}$  of the input laser is much smaller than  $\kappa$ , to a good approximation, we have  $S_{in} = I_{in} \delta(\omega)$  so that  $\eta_c(\omega) \frac{\kappa}{(\omega - \omega_c)^2 + \kappa^2} \otimes S_{in}(\omega) = I_{in} \eta_c(\omega) \frac{\kappa}{(\omega - \omega_c)^2 + \kappa^2}$ . As a result, the PL spectrum  $I_{PL}(\omega)$  is a Lorentzian profile modulated by the occupation of free electrons  $\eta_e(\omega)$ .

To compare our model and the experiment results, we rewrite the scattering and PL spectra as a function of the wavelength. The scattering spectra has a Lorentzian profile and simply takes the form

$$I_{SC}(\lambda) = A' I_{in} \eta_D(\lambda) \frac{\delta \lambda_c^2}{(\lambda_c^2 / \lambda - \lambda_c)^2 + \delta \lambda_c^2}, \quad (8)$$

where  $A' = \frac{4\langle \cos^2 \beta \rangle \langle \cos^2 \theta \rangle \eta_c^2(\omega_{in}) \kappa_{ex1} \kappa_{ex2}}{\kappa^2 \pi}$  is a constant,  $\lambda_c = \frac{2\pi c}{\omega_c}$  is the light wavelength corresponding to the resonance frequency  $\omega_c$  of the plasmon mode with the light velocity  $c$  and  $\delta \lambda_c = \frac{\kappa}{\omega_c} \lambda_c$  the linewidth of the radiation due to the LSPR mode in nm. Thus,  $I_{SC}(\lambda)$  is a Lorentzian profile modulated by the quantum efficiency  $\eta_D(\omega)$ .

In contrast to the scattering spectrum, the PL spectrum is dependent on the occupation of free electrons  $\eta_e(\omega)$  and has the form

$$I_{PL}(\lambda) = A I_{in} \cos^2 \beta \cos^2 \theta \eta_c(\lambda_{in}) \eta_D(\lambda) \eta_e(\lambda) \times \frac{\delta \lambda_c^2}{(\lambda_c^2 / \lambda_{in} - \lambda_c)^2 + \delta \lambda_c^2} \frac{\delta \lambda_c^2}{(\lambda_c^2 / \lambda - \lambda_c)^2 + \delta \lambda_c^2}, \quad (9)$$

where  $A = \frac{4\kappa_{ex1} \kappa_{ex2}}{\kappa^2 \pi} \frac{\langle H_{COoFE} | H_{photon} \rangle^2}{|H_{COoFE}|^2 |H_{photon}|^2}$  is a constant.  $\lambda_{in} = \frac{2\pi c}{\omega_{in}}$  is the wavelength of the input cw laser field. Here the FESD is rewritten as

$$\eta_e(\lambda) = N_{FE} / (1 + e^{\tau_T (\lambda_\mu / \lambda - 1)}), \quad (10)$$

where  $\lambda_\mu = 2\pi c / \mu$  is the corresponding light wavelength of the chemical potential and  $\tau_T = \hbar \mu / K_B T$  is a transition energy related to  $K_B T$ . Because the electrons gain the energy of  $\hbar \omega_{in}$ , we have the chemical potential  $\mu \approx \omega_{in}$  yielding  $\lambda_\mu \approx \lambda_{in}$ . Our experimental observations and the reported results by others [12, 18] support this suggestion. Thus  $\eta_e(\omega_{in}) = 0.5 N_{FE}$ . Later we will study the dependence of the parameter  $\tau_T$  on the input power.

Interestingly, The formula Eq. 9 immediately provides an explanation of the aspect-ratio dependence of PL emission discussed by Mohamed et al. [2, 33]. According to our model and Eq. 9, like an optical cavity, the peak position  $\lambda_c$  (resonance wavelength) of PL emission increase linearly as the nanorod length  $L$  increasing. Note that this effective length  $L$  corresponds to the mode volume of the one-dimensional nanoresonator.  $\eta_c(\omega)$  is a linear function of  $|H_{COoFE}|^2$  which is proportional to the number  $N_{FE}$  of free electrons in nanorods. In a gold nanorod, it is reasonable to assume that  $N_{FE}$  is proportional to the length of nanorod. Thus, the quantum efficiency corresponding to  $I_{PL}$  increase quadratically as a function of the length because  $\eta_c(\omega_{in}) \eta_c(\omega) \propto N_{FE}^2$ . These predictions agree well with experiments [1, 2, 33] and Mohamed's model as well [2, 33]. As the length increases further, the active number of free electrons becomes saturate due to the temporal and spatial correlation limited by the free path effect of electrons [34]. On the other hand, the PL can be saturate as increasing the input power when the excitation laser activates all free electrons. This kind of saturation has been observed in others experiments [6, 9] and our observation as well [19].

According to our model, the detected PL has the features as follows: (i) The PL intensity is a linear function of the intensity of the input laser field; (ii) The PL intensity depends on both of the polarization of the input laser field and that of the LSPR mode. It is modulated by the function of  $\cos^2(\theta)$ ; (iii) The PL intensity is dependent on the detuning between the driving laser field and the LSPR mode; (iv) The PL is Lorentzian profile modulated by the quantum efficiency  $\eta_D$ , the FESD  $\eta_e$ . (v) The PL emission becomes saturate when the input power excites all  $N_{FE}$  free electrons to a collective oscillation [6, 9, 19]. (vi) the PL efficiency is dependent on the aspect ratio of the nanorods.

Our model can also explain the enhanced quantum yield (QY) of gold nanoparticles rather than the bulk materials. To estimate the QY we assume a constant decay rate  $\kappa$  and the

external coupling rates  $\kappa_{ex1}$  and  $\kappa_{ex2}$  for simplicity although it is observed in experiments to be dependent on the length of nanorods. We consider the integral spectrum from a low enough boundary  $\omega_{cut} \approx 1.424$  eV corresponding to 869 nm to  $\omega_{in}$  for the Stokes PL emission and from  $\omega_{in}$  to  $+\infty$  for the anti-Stokes PL. The QY can be evaluated as

$$QY_S(\omega_{in}, L) = \frac{BL^2\kappa^2}{(\omega_{in} - \omega_c(L))^2 + \kappa^2} \times \int_{\omega_{cut}}^{\omega_{in}} \frac{\kappa\eta_c(\omega, \omega_{in})}{(\omega - \omega_c(L))^2 + \kappa^2} d\omega, \quad (11)$$

for the Stokes PL, and

$$QY_{AS}(\omega_{in}, L) = \frac{BL^2\kappa^2}{(\omega_{in} - \omega_c(L))^2 + \kappa^2} \int_{\omega_{in}}^{+\infty} \frac{\kappa\eta_c(\omega, \omega_{in})}{(\omega - \omega_c(L))^2 + \kappa^2} d\omega, \quad (12)$$

for the anti-Stokes PL.  $B$  is a scale coefficient. In  $\eta_c(\omega)$  the parameter  $\mu$  is replaced by  $\omega_{in}$ . The value of  $\omega_{cut}$  is not crucial and it can be smaller or larger. For a bulk film the total number of the active free electrons  $N_{FE,Bulk}$  are constant because the free electrons have a limited correlation length. To provide a rough estimation, we assume that  $N_{FE,Bulk}$  corresponds to a length  $L_{max} = 50$  nm. Then the QY of the PL from a bulk material is roughly given by

$$QY_{Bulk}(\omega_{in}, L) = \frac{BL_{max}^2\kappa^2}{(\omega_{in} - \omega_c(L))^2 + \kappa^2} \times \int_{\omega_{cut}}^{\omega_{in}} \frac{\kappa\eta_c(\omega, \omega_{in})}{(\omega - \omega_c(L))^2 + \kappa^2} d\omega. \quad (13)$$

It can be roughly evaluated as  $QY_{Bulk}(\omega_{in}, L \rightarrow \infty)$ .

Now we test the validity of our model by fitting the scattering and PL spectra observed in our experiments. The quantum efficiency of the detector used in experiment can be nearly perfect fitted by a polynomial function  $\eta_D(\lambda) = -8.87998 \times 10^{-11}\lambda^4 + 2.3287 \times 10^{-7}\lambda^3 - 2.3242 \times 10^{-4}\lambda^2 + 0.10378\lambda - 16.421$  with  $\lambda$  has the unit of nm.

### III. EXPERIMENTAL MEASUREMENT

Note that the scattering spectra are created by the unpolarized, weak white light shedding on the gold nanorod. The white light has a very broad and flat spectra over 500 nm to 800 nm. As predicted by Eq. 8, the scattering spectra have Lorentzian profiles. Our formula Eq. 8 perfectly reproduces the observed scattering spectra shown in Figs. 2 (a) and (b).

In contrast to the scattering, a cw laser field at 632.8 nm was applied to excite the PL emission. Because the power,  $I_{in}$ , and wavelength,  $\lambda_{in} = 632.8$  nm, of the excitation laser in experiments are fixed, we fit all PL spectra using the same function for FESD,  $\eta_e(\lambda) = N_{FE}/(1 + e^{\tau_T(\lambda_\mu/\lambda - 1)})$  with  $\lambda_\mu = 633$  nm and  $\tau_T = 65$ . For the Stokes component, the FESD distribution is flat approximately and the PL emission is dominated by the LSPR mode. As a result, the Stokes spectrum has Lorentzian profiles. Remarkably, the anti-Stokes

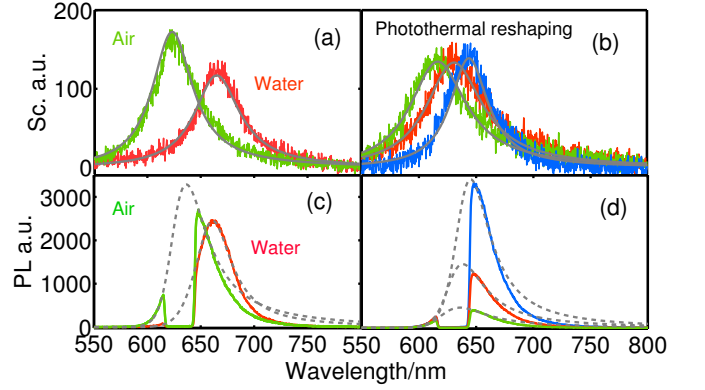


FIG. 2. (Color online) Light emission spectra as the local surface plasmon resonant frequencies being changed. (a) and (c) The scattering and PL spectra of the same nanorod by changing the refractive index in situ. (b) and (d) The scattering and PL spectra of the single individual nanoparticle being reshaped through photothermal effect. All spectra were recorded after photothermal reshaping with the same excitation intensity. To use the y-axis ticks in (c), the PL spectra in (d) is scaled by a factor of 2.

components are dominated by  $\eta_e(\lambda)$ , which is the Fermi-Dirac distribution multiplied by the total number of free electrons  $N_{FE}$ . It can be clearly seen that both the anti-Stokes and Stokes spectra of the PL in Figs. 2 (c) and (d) are well fitted by Eq. 9 of our model. All parameters for fitting are listed in the supplementary information.

The constant factors  $A'\kappa^2$  and  $A\kappa^3$  for the scattering and the PL spectra are close when we change the refractive index in situ. Their relative difference is about 30% and can attribute to the change of the polarization of the LSPR mode and the absorption of environment. The cases for the reshaped nanorods are essentially different. The wavefunction  $|H_{CoFe}\rangle$  and the polarization  $\vec{d}$  of the LSPR mode are crucially dependent on the shape of nanoparticles, whereas the input laser field is linear-polarized and has a fixed mode profile  $|H_{photon}\rangle$ . As a result, the factors  $A\kappa^3$  in the PL spectra changes considerably during reshaping.

Our model provides a unified understanding of the experimental observation for both the anti-Stokes and Stokes PL emission. It reveals that the quantum occupation of free-electron state  $\eta_e(\omega)$  in the thermal equilibrium essentially modifies the anti-Stokes components of the PL emission from a single gold nanorod. We note that the anti-Stokes radiation has been reported as a result of the thermal radiation [16] or the thermal population of the electron-hole excitations during Raman scattering [9]. However, it is improper to attribute the PL emission observed in our experiment to the thermal radiation. The thermal radiation from a black body [16] is unpolarized and must be polarization-independent. On the contrary, the PL intensity in our experiment is crucially dependent on the polarization of the exciting laser and the collection polarization of the detector [19]. Moreover, the polarization dependence of the anti-Stokes emission is strongly correlated to that of the Stokes emission. It implies that the anti-Stokes and the Stokes emission in our experiment share a mechanism fun-

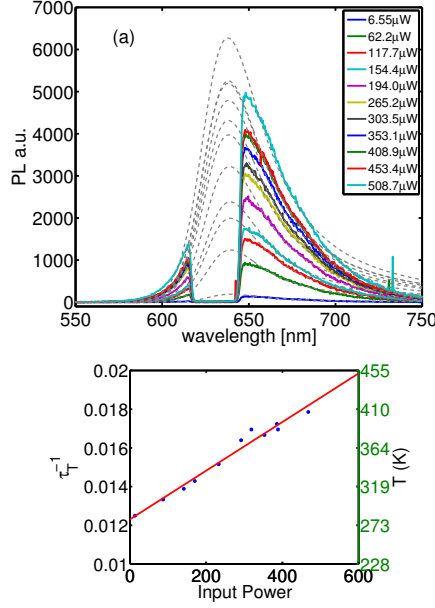


FIG. 3. (a) Fitting the PL spectra from a single gold nanorod excited by a cw laser with different power  $P_{in}$ . To fit the data, we have scaled the input power by a factor  $\sim 1$ . (b) Dependence of the parameter  $\tau_T$  and the local temperature  $T$  in the FESD  $\eta_e(\omega)$  as a function of the input power.  $\lambda_\mu = 633$  nm.

damentally different from the thermal radiation. Besides, the model based on the thermal distribution of the electron-hole excitation only explain the anti-Stokes emission with a large Raman shift [9]. The discrepancy between the model and the experimental observation results to the deviation at the Stokes emission and even at the anti-Stokes near the excitation frequency can be one order [9]. A weak anti-Stokes PL has been observed in the PL of a single gold nanoparticle by Beversluis et al. [29], but an explanation is lack. Here we present a self-consistent and unified model in good agreement with both the anti-Stokes and Stokes components in the PL from a single gold nanorod.

An interesting parameter in our model is  $\tau_T$  corresponding to the nanoscale-localized temperature. We studied the dependence of  $\tau_T$  on the input power by fixing the frequency of cw excitation. We increased the power of the laser by two orders from  $\sim 7$   $\mu$ W to  $\sim 500$   $\mu$ W. By fitting the experimental data shown in Fig. 3 (a), we find a relation  $\tau_T^{-1}$  corresponding to the nanoscale-localized temperature  $T$  increases linearly as  $P_{in}$  increases (see Fig. 3 (b)), where  $P_{in}$  is the power of the excitation laser. Note that the maximal temperature of our samples is below 410 K. Such low temperature can not support an effective thermal luminescence at the visible light frequency.

#### IV. THEORETICAL PREDICTION

The quantum yield (QY) of the PL from noble metal nanoparticles is a few orders higher in amplitude in compar-

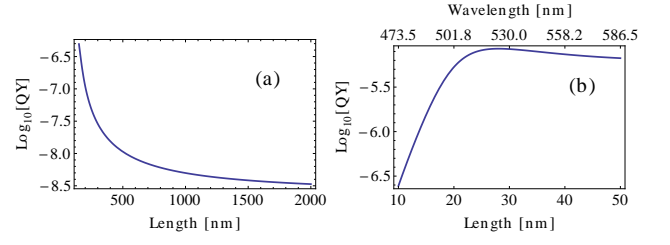


FIG. 4. Quantum yield of the PL emission from (a) a bulk material or (b) a single gold nanorod. Other parameters are  $\omega_{in} = 2.474$  eV,  $\tau_T = 65$ . For simplicity, we fix  $\kappa = 0.123$  eV. To provide a quality reproduction of the measurement [1], we simply assume a linear relation  $\lambda_c = 530\text{nm} + 2.82(L - 30\text{nm})$  as an example [2]. Note that this relation depends on the shape of the samples.

ison with bulk film [2, 3, 14, 35] and has shape-dependence [2, 14, 33]. However, “no explanation was proposed for the larger QY of nanorods and its shape dependence.” and the origin of the saturation of the PL QY is unknown [14]. Our model may provide a understanding to the origin of the enhanced QY and the saturation phenomenon.

Now we compare the QYs between a single nanorod and a bulk film. We consider the bulk film as a long nanorod with a very small  $\omega_c(L) \ll \omega_{in}$ . Therefore, at a given detection frequency  $\omega$ , the ratio of the PL intensity between the single nanorod and the bulk film is roughly  $\omega_{in}^2 \omega^2 / [(\omega_{in} - \omega_c(L))^2 + \kappa^2] [(\omega - \omega_c(L))^2 + \kappa^2]$  ( $\omega_{in}, \omega \gg \kappa$ ). When  $\omega_{in} \sim \omega_c(L)$  and  $\omega \sim \omega_c(L)$ , the ratio is largest and can be the order of  $Q^4$  with  $Q = \omega_c(L)/\kappa$  is the quality factor of the scattering spectrum. A mediate quality factor  $Q = 20$  already yields a ratio of  $1.6 \times 10^5$ . According to our model, the high PL QY of noble metal nanorods origins from the enhancement of the excitation and emission due to the resonance plasmonic resonator similar to the case that the optical cavity greatly increase the localized optical field.

The QY as a sum of the PL spectrum is dependent on the length of nanorods. In Fig. 4, we numerically calculate the QY for single nanorods and a bulk film. Clearly, the QY of a bulk film can be as low as  $10^{-8.5}$  and that of a single nanorod can two to three orders higher. More importantly, our model correctly predicts the observed saturation of the QY of the PL from a single gold nanorod [14] even without taking into account the free path effect of the electrons [34]. We find that the QY increases first when  $L$  is small and then becomes saturate at  $\sim L_s = 25$  nm. Note that the saturation length  $L_s$  is dependent on the specific function  $\lambda_c(L)$ .

According to Eqs. 11 and 12 both the anti-Stokes and Stokes components of the PL QY are dependent on the excitation frequency  $\omega_{in}$ . It can be seen from Fig. 5 that both components increase first and then decrease as the excitation frequency increases. When the excitation matches the resonance frequency of the plasmonic resonator  $\omega_c$ , both the anti-Stokes and Stokes reach the peak. However, the anti-Stokes emission is always smaller than the Stokes one. The largest ratio between two components is about 0.22 at  $\omega_{in} = 0.95\omega_c$ .

We are aware of that the PL spectrum from gold nanorods are normally complex in experiments and may has more than

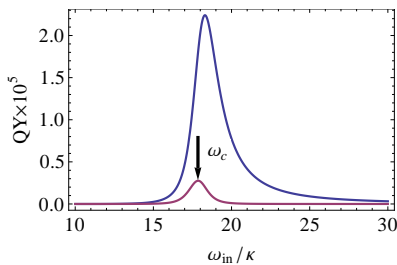


FIG. 5. Quantum yield of the anti-Stokes and Stokes components and the PL emission from a single gold nanorod as a function of the excitation frequency. Other parameters are  $\hbar\omega_c = 2.22$  eV,  $\kappa \approx 0.123$  eV,  $\tau_T = 65$ .

one resonance peak. However, our theory presents a simple but basic concept for understanding the main features of the one-photon luminescence from gold nanorods.

## V. CONCLUSION

In summary, we have experimentally observed the one-photon luminescence emission from a single gold nanorod. Based on experimental observations, we have presented a uni-

fied theoretical model to explain both the anti-Stokes and Stokes spectral components although their profiles are substantially different. The Stokes component has Lorentzian profile and origins mainly from the resonant emission of the plasmonic nanoresonator, while the anti-Stokes PL is the result of the radiation from the plasmonic nanoresonator modulated strongly by the redistribution of the free electrons. The light emission process is determined by both the cavity resonance and electron distribution. Our model also provides a self-consistent explanation for the polarization and size dependence of the one-photon luminescence from a single gold nanorod. In particular, it predicts the enhanced quantum yield and the saturation of the QY. Our theory provides a new view angle to understand the photoluminescence emission process from noble metal nanoparticles.

## ACKNOWLEDGEMENT

This work was supported by the National Key Basic Research Program of China (grant No. 2013CB328703) and the National Natural Science Foundation of China (grant Nos. 11204080, 11374026, 11121091, 91221304). K.X. also thanks for the support by the Australian Research Council Centre of Excellence for Engineered Quantum Systems (EQuS), project number, CE110001013.

- 
- [1] M. Yorulmaz, S. Khatua, P. Zijlstra, A. Gaiduk, and M. Orrit, *Nano Lett.* **12**, 4385 (2012).
  - [2] M. B. Mohamed, V. Volkov, S. Link, and M. A. El-Sayed, *Chem. Phys. Lett.* **317**, 517 (2000).
  - [3] E. Dulkeith, T. Niedereichholz, T. A. Klar, J. Feldmann, G. von Plessen, D. I. Gittins, K. S. Mayya, and F. Caruso, *Phys. Rev. B* **70**, 205424 (2004).
  - [4] T. Zhang, G. Lu, H. Shen, K. Shi, Y. Jiang, D. Xu, and Q. Gong, *Sci. Rep.* **4**, 3867 (2014).
  - [5] H. Wang, T. B. Huff, D. A. Zweifel, W. He, P. S. Low, A. Wei, and J.-X. Cheng, *PNAS* **102**, 15752 (2005).
  - [6] S.-W. Chu, T.-Y. Su, R. Oketani, Y.-T. Huang, H.-Y. Wu, Y. Yonemaru, M. Yamanaka, H. Lee, G.-Y. Zhuo, M.-Y. Lee, S. Kawata, and K. Fujita, *Phys. Rev. Lett.* **112**, 017402 (2014).
  - [7] G. Lu, J. Liu, T. Zhang, W. Li, L. Hou, C. Luo, F. Lei, M. Manfait, and Q. Gong, *Nanoscale* **4**, 3359 (2012).
  - [8] T. Zhang, H. Shen, G. Lu, J. Liu, Y. He, Y. Wang, and Q. Gong, *Adv. Opt. Mater.* **1**, 334 (2013).
  - [9] J. Huang, W. Wang, C. J. Murphy, and D. G. Cahill, *PNAS* **111**, 906 (2014).
  - [10] G. Lu, L. Hou, T. Zhang, J. Liu, H. Shen, C. Luo, and Q. Gong, *J. Phys. Chem. C* **116**, 25509 (2012).
  - [11] M. S. Tame, K. R. McEnery, S. K. Özdemir, J. Lee, S. A. Maier, and M. S. Kim, *Nature Phys.* **9**, 329 (2013).
  - [12] A. Tcherniak, S. Dominguez-Medina, W. Chang, P. Swanglap, L. S. Slaughter, C. F. Landes, and S. Link, *J. Phys. Chem.* **115**, 15938 (2011).
  - [13] O. P. Varnavski, T. Goodson, M. B. Mohamed, and M. A. El-Sayed, *Phys. Rev. B* **72**, 235405 (2005).
  - [14] M. Yorulmaz, S. Khatua, P. Zijlstra, A. Gaiduk, and M. Orrit, *Nano Lett.* **12**, 4385 (2012).
  - [15] Y.-N. Hwang, D. H. Jeong, H. J. Shin, D. Kim, S. C. Jeoung, S. H. Han, J.-S. Lee, and G. Cho, *J. Phys. Chem. B* **106**, 7581 (2002).
  - [16] M. B. Agranat, A. A. Benditskiĭ, G. M. Gandel'man, P. S. Kondratenko, B. I. Makshantsev, G. I. Rukman, and B. M. Stepanov, *Sov. Phys. JETP* **52**, 27 (1980).
  - [17] M. B. Agranat, A. A. Benditskiĭ, G. M. Gandel'man, A. G. Devyatkov, P. S. Kondratenko, B. I. Makshantsev, G. I. Rukman, and B. M. Stepanov, *JETP Lett.* **30**, 167 (1980).
  - [18] M. R. Beversluis, A. Bouhelier, and L. Novotny, *Phys. Rev. B* **68**, 115433 (2003).
  - [19] Y. He, K. Xia, G. Lu, H. Shen, Y. Cheng, Y. chun Liu, K. Shi, Y.-F. Xiao, and Q. Gong, (submitted).
  - [20] J. Nelayah, M. Kociak, O. Stéphan, F. Javier García de Abajo, M. Tencé, L. Henrard, D. Taverna, I. Pastoriza-santos, L. M. Liz-Marzán, and C. Colliex, *Nature Phys.* **3**, 348 (2007).
  - [21] F. P. Schmidt, H. Ditlbacher, F. Hofer, J. R. Krenn, and U. Hohenester, *Nano Lett.*, 10.1021/nl502027r (2014).
  - [22] K. Xia and J. Twamley, *Phys. Rev. X* **3**, 031013 (2013).
  - [23] M. Bora, B. J. Fasenfest, E. M. Behymer, A. S.-P. Chang, H. T. Nguyen, J. A. Britten, C. C. Larson, J. W. Chan, R. R. Miles, and T. C. Bond, *Nano Lett.* **10**, 2832 (2010).
  - [24] Z. Sun and D. Zeng, *J. Opt. Soc. Am. B* **24**, 2883 (2007).
  - [25] J. Hohlfield, S. S. Wellershoff, J. Güdde, U. Conrad, V. Jähnke, and E. Matthias, *Chem. Phys.* **251**, 237 (2000).
  - [26] F. T. Boyd, Z. H. Yu, and Y. R. Shen, *Phys. Rev. B* **33**, 7923 (1986).
  - [27] K. Xia, *Phys. Rev. A* **89**, 023815 (2014).
  - [28] K. Xia, G. K. Brennen, D. Ellinas, and J. Twamley, *Opt. Express* **20**, 27198 (2012).

- [29] M. R. Beversluis, A. Bouhelier, and L. Novotny, Phys. Rev. B **68**, 115433 (2003).
- [30] M. J. Collett and C. W. Gardiner, Phys. Rev. A **30**, 1386 (1984).
- [31] C. W. Gardiner and M. J. Collett, Phys. Rev. A **31**, 3761 (1985).
- [32] M. Lax, Phys. Rev. **172**, 350 (1968).
- [33] Y. Fang, W.-S. Chang, B. Willingham, P. Swanglap, S. Dominguez-Medina, and S. Link, ACS Nano **6**, 7177 (2012).
- [34] R. N. Stuart, F. Wooten, and W. E. Spicer, Phys. Rev. Lett. **10**, 7 (1963).
- [35] J. P. Wilcoxon, J. E. Martin, F. Parsapour, B. Wiedenman, and D. F. Kelley, J. Chem. Phys. **108**, 9137 (1998).